ELSEVIER

Journal of Power Sources 83 (1999) 93–99

JOURNAL OF POWER SOURCES

www.elsevier.com/locate/jpowsour

Application of electrochemical noise analysis to the study of batteries: state-of-charge determination and overcharge detection

S. Martinet [a,*], R. Durand [a], P. Ozil [a], P. Leblanc [b], P. Blanchard [c]

[a] *Laboratoire d'Electrochimie et de Physicochimie des Matériaux et Interfaces, E.N.S. d'Electrochimie et d'Electrométallurgie, 1130 Rue de la Piscine, B.P. 75, 38402 Saint-Martin d'Hères, France*

[b] *SAFT Research Department, Route de Nozay, 91460 Marcoussis, France*

[c] *SAFT Advanced Industrial Battery Group, 111-113 Boulevard A. Daney, 33074 Bordeaux Cedex, France*

Received 16 March 1999; accepted 30 March 1999

Abstract

For the first time, electrochemical noise has been studied for different types of battery under galvanostatic conditions. First, ENA has been applied successfully to sealed Ni–MH batteries: (i) for low capacities, the noise level gives an estimate of the battery state-of-charge, (ii) for high capacities (up to 93 A h), overcharge detection is achieved simultaneously or prior to other known end-of-charge criteria such as voltage and temperature derivatives. Secondly, ENA has been evaluated for overcharge detection of Ni–Cd or Li-ion batteries: (i) similar results to Ni–MH batteries are obtained for Ni–Cd technology, (ii) for Li-ion batteries, ENA measurements not only allow overcharge detection but also provide an estimate of the gas evolution rate. This technique could be extended to other batteries producing gas during working or overcharging, such as lead–acid batteries.

Keywords: Noise; Battery; State-of-charge; Overcharge; Alkaline; Lithium

1. Introduction

Many studies [1–12] have been devoted to electrochemical noise caused by different phenomena such as bubble evolution [1–4], electrode corrosion [5–11] and passivation [12]. The previous work only concerns small-sized electrodes, with surfaces typically ranging from 10^{-4} to a few square centimeters. Electrochemical Noise Analysis (ENA) has never, to our knowledge, been applied to batteries.

Nevertheless, many types of battery experience gas evolution, the main cause of electrochemical noise. For alkaline and lead–acid batteries, oxygen evolution and even hydrogen evolution are side reactions at the end-of-charge. Thus, there is a clear interest in detecting the beginning of gas evolution during battery charging. Moreover, such a detection can provide information concerning the battery state-of-charge.

For lithium batteries, there is no gas evolution during normal operating conditions. But in the case of overcharge, electrolyte or gassing agent such as lithium carbonate may be oxidised and induce gas evolution (mainly hydrocarbons, hydrogen and carbon monoxide and dioxide) [13]. In this particular case, ENA could give useful information and may be applied for the safety study of lithium-ion or lithium-polymer batteries.

The scope of this paper was to evaluate how ENA could be applied to different types of batteries (Ni–Cd, Ni–MH, Li-ion) having capacities ranging from 1.6 A h up to 100 A h. In the first part, the electrochemical noise of sealed Ni–MH batteries was studied: (i) variations with the battery state-of-charge, (ii) ability for overcharge detection in comparison with other known end-of-charge criteria such as voltage and temperature derivatives. Then, these results were extended to other systems such as Ni–Cd and Li-ion technologies.

2. Experimental

Two types of experiments were carried out: (i) investigation of electrochemical noise with state-of-charge for capacities less than 2 A h, (ii) detection of overcharge for higher capacities up to 100 A h.

* Corresponding author. Fax: +33-4-76-826577; E-mail: sebastien.martinet@lepmi.inpg.fr

0378-7753/99/$ - see front matter
PII: S0378-7753(99)00272-4

Measurements were performed in galvanostatic mode. The battery voltage signal was cleared of its DC component and amplified by an EG&G model 113 pre-amplifier. It must be noticed that measurements could have been performed at constant voltage, with a follow-up of current fluctuations.

The amplified signal was monitored and stored by a 3091 Nicolet oscilloscope. Data processing was carried out by a PC via a GPIB interface (Fig. 1). For measurement channel setting, a particular care was taken over generating a low parasitic background noise.

Data processing was achieved with a FFT program, leading to a calculation of power spectral density (psd) of voltage fluctuations. Noise Power was computed as the integral of voltage fluctuation psd between the frequency limits.

The characteristics of the batteries tested are listed in Table 1. Rated capacities are given in A h (ampere × hour).

2.1. State-of-charge determination

Tests were run upon a portable battery: a sealed 1.6 A h cylindrical Ni–MH battery referred as type A.

Since only low currents were needed for experiments (320 mA at 0.2 C rate), a lead–acid battery was used to apply a constant current to the tested battery A in series with a resistance.

The entire electrical circuit was placed in a Faraday cage to minimise parasitic noise.

A preliminary experiment consisted in measuring the electrochemical noise during a continuous charge of type A battery at 0.1 C rate. Measurements were achieved without any interruption of the charge, voltage fluctuations being processed after the experiment.

Nevertheless, the battery state-of-charge could not be deduced from charge duration as overcharge reactions

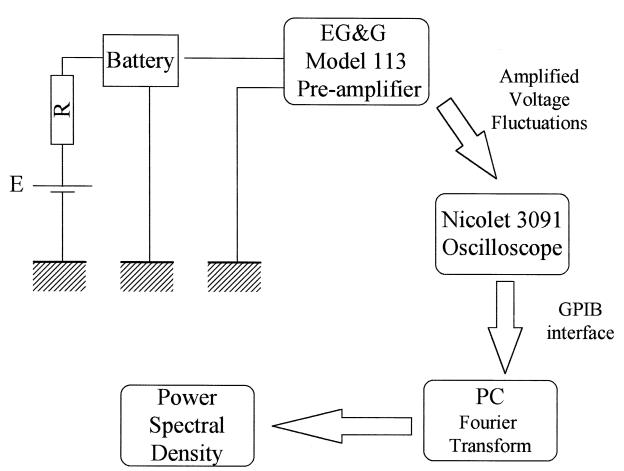

Fig. 1. Experimental set-up for ENA of battery voltage fluctuations in galvanostatic conditions. Resistance value is adjusted to monitor imposed current. For high current values, system (E,R) is replaced by a constant current supply.

Table 1
Characteristics of tested batteries

Type	Battery	Rated capacity (A h)
A	Cylindrical Ni–MH	1.6 (1.2 V)
B	Ni–MH electric vehicle module	93 (12 V[a])
C	Ni–Cd module	18 (12 V)
D	Ni–Cd electric vehicle module	100 (6 V)
E	Li-ion medium prismatic cell	1.8 (3.6 V)

[a] ENA measurements performed on a single 1.2 V cell.

significantly reduce charge efficiency at the end-of-charge. Therefore, a full discharge of the battery was necessary to get a precise value of state-of-charge.

The following procedure was used to test the ability of ENA to determine battery state-of-charge:

- battery A was charged × hours at 0.2 C rate with a Tacussel PGP201 potentiostat
- a fast ENA was performed at 0.2 C rate (less than 5 min, i.e., 2% of charge) using the lead–acid battery as a current supply, to generate low parasitic background noise
- battery A state-of-charge was measured by a full discharge at 0.2 C rate down to 1 V.

2.2. Overcharge detection

Tests were performed upon four types of batteries, three alkaline batteries and one Li-ion battery: (i) a sealed 93 A h Ni–MH electric vehicle (EV) module (type B), (ii) two Ni–Cd batteries with increasing capacities, a 18 A h Ni–Cd pack (type C) and a 100 A h Ni–Cd (type D) EV module, (iii) a 1.8 A h Li-ion ($LiCoO_2$/LiC) MP144350 cell (type E).

For overcharge detection in cases (i) and (ii), the experimental set-up was different since high current values were needed, up to 50 A. In these cases, different types of constant current supplies were used depending on the current range.

EV modules were equipped with Iron/Constantan thermocouples to provide an approximate measurement of the internal temperature of the battery.

The fully discharged battery was charged at constant current while electrochemical noise measurements were performed. The duration of voltage fluctuation records varied from about 10 min for slow charging rates (0.1 C rate, 0.2 C rate) to less than 1 min for the fastest rates (0.5 C rate, C rate).

Tests on alkaline batteries were run to detect gas evolution during normal charging, i.e., a total charged capacity between 1 and 1.5 times the nominal capacity. Detection with ENA was compared with other known end-of-charge criteria.

For the Li-ion battery, the medium prismatic cell was placed in a sealed vessel equipped with a pressure sensor. Both internal pressure variations and electrochemical noise

were recorded during a 0.1 C rate overcharged up to 3.5 A h for a rated capacity of 1.8 A h.

3. Results and discussion

3.1. ENA applied to sealed Ni–MH batteries

For Ni–MH batteries, the following reactions are in competition at the end-of-charge.

At the positive electrode:

(i) active material oxidation, $Ni(OH)_2 + OH^- \rightarrow Ni(OOH) + H_2O + e^-$

(ii) oxygen evolution, $4OH^- \rightarrow 2H_2O + O_2 + 4e^-$

and at the negative electrode:

(iii) active material reduction, $M + xH_2O + xe^- \rightarrow MH_x + xOH^-$

(iv) oxygen reduction, $2H_2O + O_2 + 4e^- \rightarrow 4OH^-$

(v) hydrogen evolution, $2H_2O + 2e^- \rightarrow 2OH^- + H_2$.

For a normal state-of-health of the battery, a sufficient negative material excess ensures that no hydrogen is evolved and reaction (v) was not to be considered. In those conditions, overcharge reactions are only oxygen recombination reactions. These reactions become significant for a battery state-of-charge close to 80% and induce strong gas evolution and bubble formation within the battery. As the electrochemical noise generated by bubbles is the most important noise source, ENA was applied to sealed Ni–MH batteries, with first tests on a small capacity battery.

3.1.1. State-of-charge determination

As previous studies available in the literature only concerned electrochemical noise for small surfaces, a preliminary experiment was performed on battery A to test the ENA ability for an electroactive positive electrode area of about 41 cm^2. The battery was charged at 0.1 C rate from the fully discharged state. ENA was performed simultaneously, with a voltage magnification from $\times 10{,}000$ at the beginning of the charge to $\times 5000$ at the end-of-charge.

During charge, the voltage fluctuation amplitude (Fig. 2a) increases from less than 1 μV to more than 10 μV. 10^{-4}% variations are detected with ENA so proving the accuracy of the analysis. Voltage fluctuations are far different from those obtained with a single electrode [2,3] which present a triangular shape, viz.:

(i) a linear increase of potential corresponding to the growth of bubbles and thus an increase of the covered electrode surface,

(ii) a steep potential drop corresponding to bubble detachments.

In our case, fluctuations correspond to the whole battery: no sharp voltage drops are observed, they are replaced by a linear voltage decrease. This observation may be explained by gas pocket growth and reduction between the two electrodes.

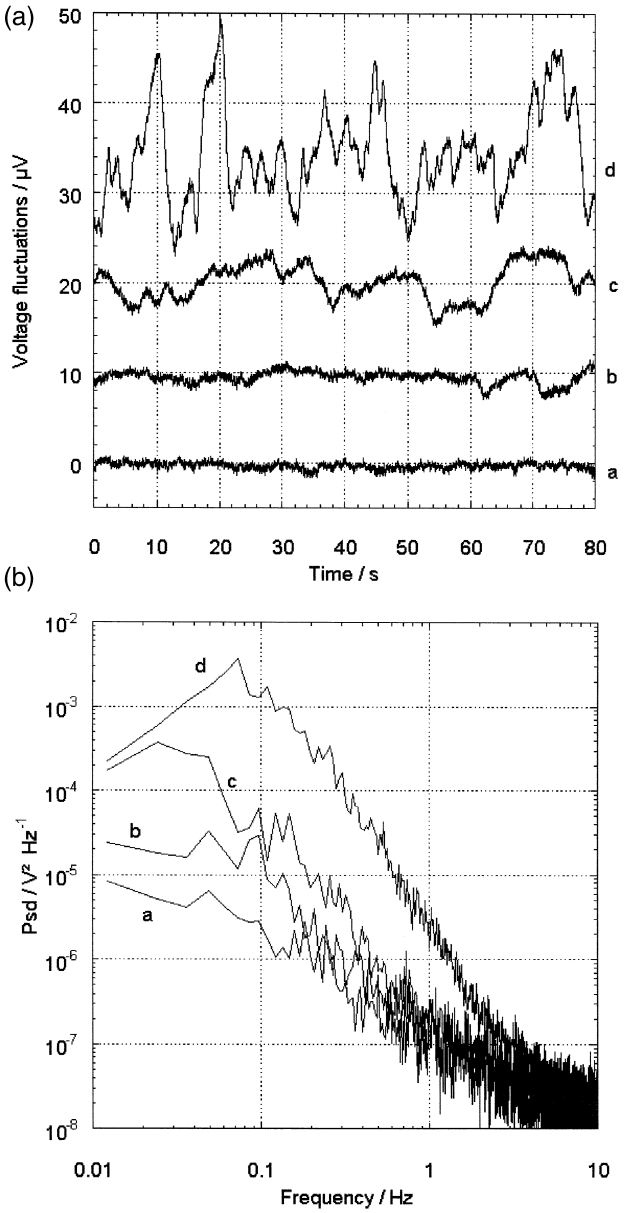

Fig. 2. Battery A at various times during charge at 0.1 C rate from fully discharged state. (a) 4 h, (b) 7 h, (c) 10 h, (d) 14 h. (a) Voltage fluctuations. (b) Voltage fluctuation power spectral densities.

As shown in Fig. 2b, power spectral density plots have two parts: a low-frequency plateau ($f < 0.1$ Hz) followed by a $f^{(-a)}$ decrease. During charge, the whole curve is shifted towards upper values while the frequency slope (a) increased from about 2 to 3. The noise power obtained with psd integration between 0.03 Hz and 25 Hz, increases strongly with charge input up to 2.24 A h (14 h charge).

In this paper, we have measured electrochemical noise at the terminals of the battery. Therefore, noise measurements include as a whole both the phenomena occurring at the electrodes and in the separator. Thus, it is rather difficult to propose an explanation for the shape either of the voltage fluctuations or of the psd, as the models previously developed by Gabrielli et al. [2,3] for a single

electrode cannot be applied a priori. Nevertheless, a further comprehensive study will be devoted to a better understanding of electrochemical noise in batteries [14] and to determine precisely its source.

ENA results of the second run on battery A were plotted as a function of the battery state-of-charge (SOC) which was determined by discharge duration. Indeed, the battery state-of-charge is different from charge input because of overcharge reactions creating a decrease in charge efficiency.

The results clearly show the correlation between noise power and SOC (Fig. 3). Between 20% and 80% SOC, noise power varies quite linearly with SOC in logarithmic scale. For SOC > 80%, noise power is significantly increased due to a strong oxygen evolution.

Thus, ENA appears to have a great interest because it can be used not only as an indicator of strong oxygen evolution, but also for discriminating state-of-charge between 20% to 80%.

ENA allows one to estimate the state-of-charge of sealed portable Ni–MH batteries and could be tested for larger capacities or for lead–acid batteries.

3.1.2. Overcharge detection

Due to experimental difficulties, such as the use of a current supply, noise measurements on battery B were much more difficult than for a smaller system such as battery A. Thus, in this case, our interest was only to demonstrate the ability of ENA to detect overcharge reactions for a 93 A h Ni–MH EV module by comparing ENA measurements with other end-of-charge criteria.

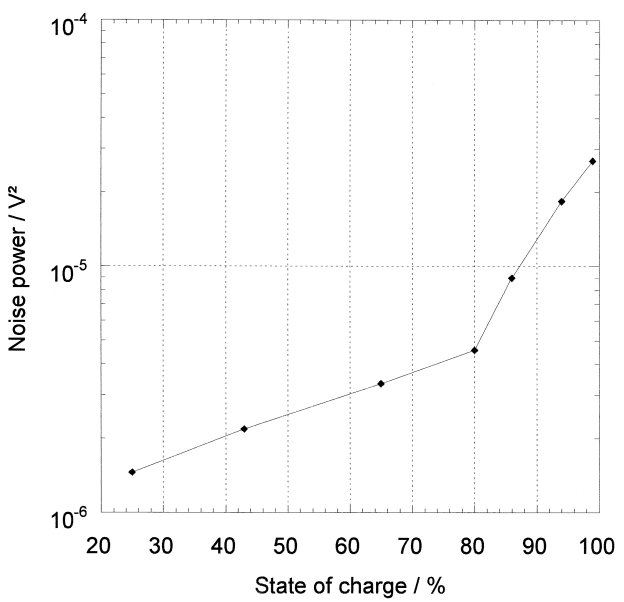

Fig. 3. ENA applied to battery A at various states-of-charge. Noise power is calculated from the integration of voltage fluctuation psd between 0.03 Hz and 25 Hz. State-of-charge of the battery is determined by a full discharge at 0.2 C rate after electrochemical noise measurement.

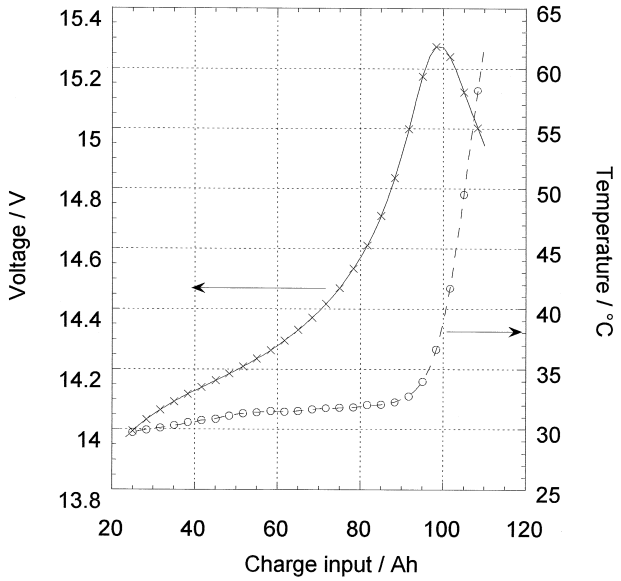

Fig. 4. Voltage and temperature monitoring during battery B continuous charge at 0.54 C rate (50 A). (×) voltage, (○) temperature.

Battery B (pack of 10 cells) was charged with a 50 A constant current up to 120% of the rated capacity. Electrochemical noise and temperature were simultaneously recorded, the total voltage of the pack was monitored during charge, but the voltage of only one cell of the pack was amplified for ENA.

The battery voltage passes through a maximal value at 15.3 V for a 98 A h charge input (Fig. 4), while the temperature rises up to 60°C at the end of overcharge.

For the cell under study, voltage oscillations of 200 μV are observed. ENA gives very interesting results between 0.5 Hz and 25 Hz compared with temperature and voltage derivatives (Fig. 5a and b, respectively).

The noise power significantly increases when the charge input exceeds 60 A h, with an exponential shape, while the temperature derivative remains constant up to 80 A h.

In the range of 20–80 A h, the noise power and the voltage derivative seem to vary in a similar way, but after the voltage peak, the voltage derivative strongly decreases towards negative values while the noise power is an increasing function of the charge input that directly traduces the extent of gas evolution.

3.2. Overcharge detection applied to Ni–Cd and Li-ion technologies

As Ni–MH results could not a priori be transposed for Ni–Cd technology, and especially not for Li-ion technology, a series of experiments was carried out on two Ni–Cd battery packs (batteries C and D) of increasing capacities and on one Li-ion medium prismatic cell (battery E).

3.2.1. Overcharge detection applied to Ni–Cd technology

Overcharge reactions for Ni–Cd batteries are similar to those of Ni–MH batteries, except for hydrogen evolution

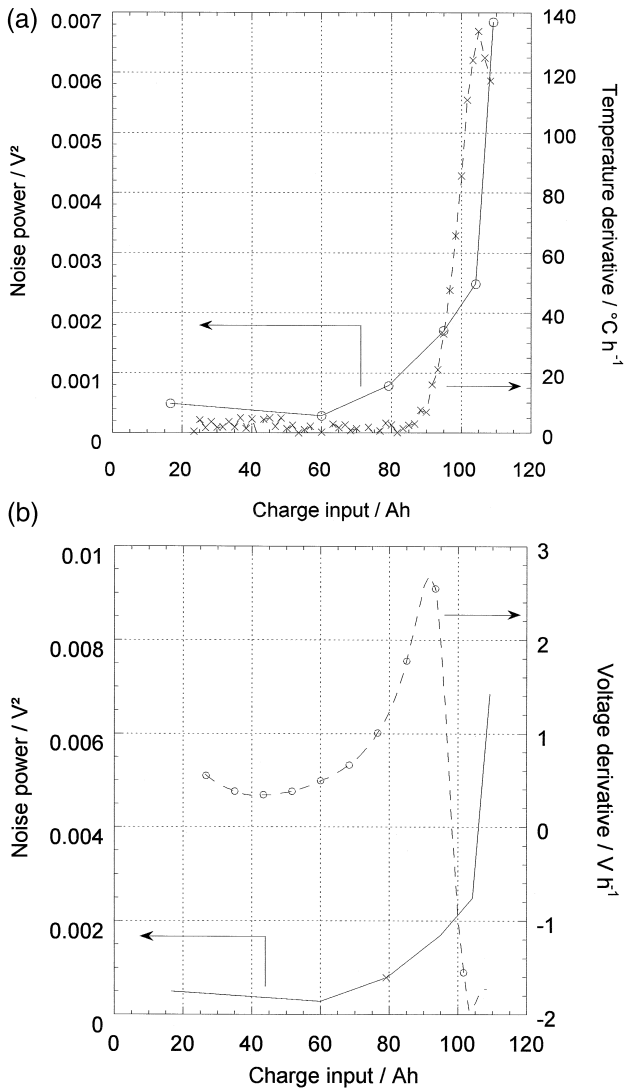

Fig. 5. Comparison between noise power (0.5 Hz to 25 Hz) and various end-of-charge criteria for battery B during 50 A charge. (a) ○, noise power; ×, temperature derivative. (b) ○, noise power; ×, voltage derivative.

that is possible only at the end of negative material charge: the hydrogen evolution overvoltage on cadmium negative electrodes is far greater than the corresponding overvoltage on MH electrodes, preventing hydrogen evolution during negative material charge. Thus, ENA results for Ni–Cd technology were expected to be quite similar to Ni–MH technology.

Battery C (18 A h rated capacity) was charged at 0.2 C rate during 7.5 h. Two types of ENA were performed to detect overcharge, one at low frequencies (0.005 Hz to 5 Hz) and the other one at higher frequencies (0.03 Hz to 25 Hz). Results plotted in Fig. 6 show a continuous increase of noise power as a function of charging time for low frequency integration of psd: this indicates once again the ability of ENA for SOC evaluation even for Ni–Cd technology and for a rather high rated capacity.

On the other hand, noise power calculated on short records (higher frequencies) exhibits peaks after 5 h. These peaks correspond to sharp fluctuations probably due to gas pockets.

Thus, a follow-up of voltage fluctuation psd in the appropriate frequency domain may be a valid way for overcharge detection:

(i) at lower frequencies, ENA seems to provide an evaluation of the gas evolution rate and thus, the end-of-charge criterion could be fixed as a critical value of the noise power,

(ii) at higher frequencies, the detection of first evolving bubbles is possible and ENA may allow one to stop charging at that moment.

The scope of further experiment was to evaluate more precisely ENA measurements as an end-of-charge criterion.

A test on a Ni–Cd EV module D was performed at 0.3 C. During the charge, the beginning of gas evolution was strongly marked after a 90 A h charge input with a voltage jump from 7.5 V to 8.5 V in a few minutes (Fig. 7).

ENA could not be applied during the voltage jump, because voltage fluctuations saturated the amplifier. However, the noise power was measured after and before this jump. During overcharge, voltage fluctuations are ever more pronounced, with an increasing frequency of appearance indicating the shift from charging reactions towards gas evolution. The voltage amplitude ranges from 0.3 mV to 1 mV for the whole 6 V pack, corresponding to signal variations between 0.005% and 0.015% detected with a standard current supply.

In Fig. 8, the comparison between the noise power and the temperature derivative once again shows that the noise

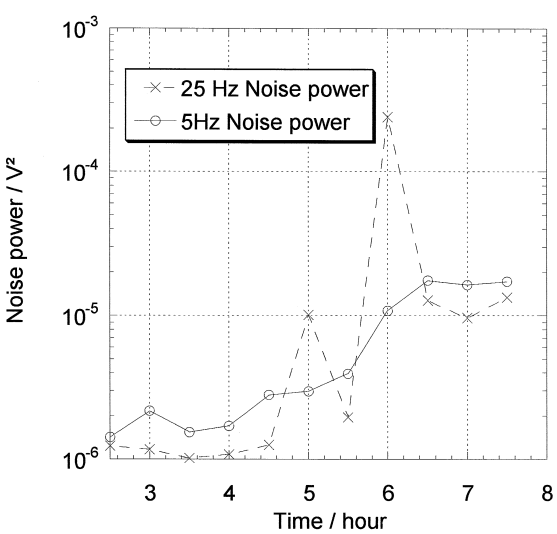

Fig. 6. ENA applied to battery C during a continuous charge at 0.2 C rate. Noise power is calculated from the integration of voltage fluctuations psd between 0.005 Hz and 5 Hz for 5 Hz curve (○) and between 0.03 Hz and 25 Hz for 25 Hz curve (– × –).

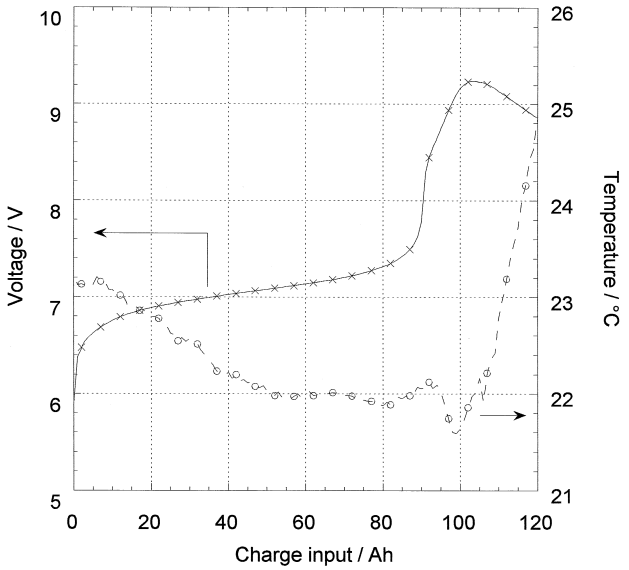

Fig. 7. Voltage and temperature monitoring during battery D continuous charge at 0.3 C rate (30 A). (×), voltage, (○), temperature.

power continuously increases and responds simultaneously with the temperature derivative which begins to increase after 95 A h.

Therefore, overcharge detection was performed with ENA measurements on a 100 A h Ni–Cd EV module and led again to similar or better results than other end-of-charge criteria.

3.2.2. Overcharge detection applied to Li-ion technology

The last experiment on Li-ion battery E had two objectives: to verify that ENA could be applied for such a type of battery and to prove from pressure measurements the correlation between the measured noise and the current fraction contributing to gas evolution.

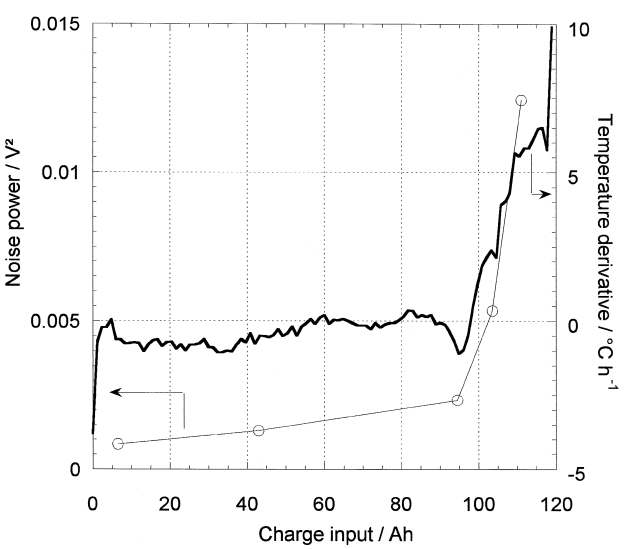

Fig. 8. Comparison between noise power (0.03 Hz to 2.5 Hz) and temperature derivative as end-of-charge criteria for battery D during 30 A charge. (○) noise power, (continuous line) temperature derivative.

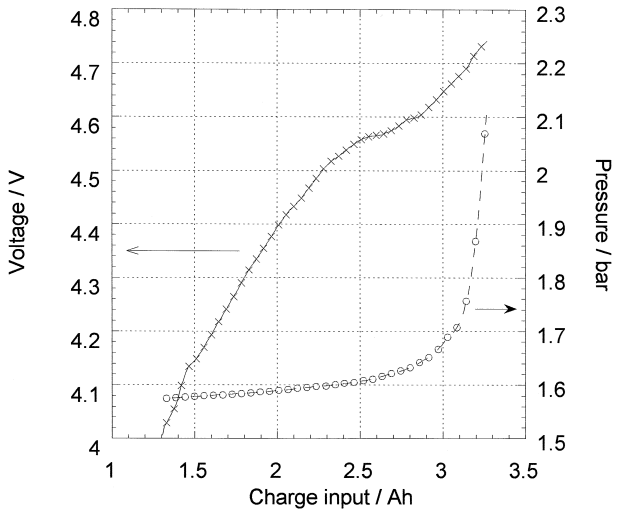

Fig. 9. Voltage and pressure monitoring during Li-ion battery E continuous charge at 0.1 C rate (0.18 A). (×) voltage, (○) pressure.

In Fig. 9, the pressure strongly increases once the charge input exceeds 3 A h. Before 3 A h, there is only little gas evolution because the positive electrode continues to provide lithium. Indeed, the electrode composition at the end of a normal charge is close to $Li_{0.45}CoO_2$.

In the experiment, a strong parasitic noise was generated by using a pressure sensor. Thus, the noise power had to be calculated in a restricted frequency domain chosen arbitrarily between 1 Hz and 2.5 Hz. For a better understanding of the significance of noise power, we have plotted this parameter as a function of the pressure derivative (Fig. 10). By using the ideal gas law, the pressure derivative is directly proportional to the current fraction (i_{gas}/i_{tot}) contributing to gas evolution (Note: experiment

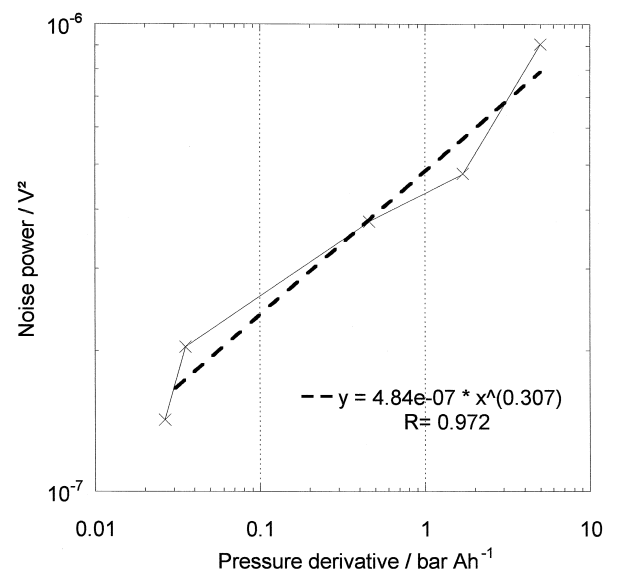

Fig. 10. Noise power (1 Hz to 2.5 Hz) plotted in function of pressure derivative for battery E during charge at 0.1 C rate. Dotted line: power of pressure derivative regression.

was run under galvanostatic conditions, and a constant number of electrons needed per mole of gas is supposed).

In those conditions, the noise power is found to be expressed as a power of the gas evolution current fraction:

$$\text{noise power}/V^2 = 6 \times 10^{-6} \left(\frac{i_{\text{gas}}}{i_{\text{tot}}} \right)^{0.3} \quad (1)$$

where constant coefficients strongly depend on experimental conditions, such as frequency limits for example.

These results clearly show that ENA offers a way to quantify overcharge reactions in batteries when these reactions produce gas.

4. Conclusion

Electrochemical noise measurements have been applied to different types of battery under galvanostatic conditions.

First, ENA allows an estimate to be made of the state-of-charge of small capacity sealed Ni–MH batteries. This could be tested more precisely for capacities higher than a few ampere-hours or for all types of battery which produce gas during working (Ni–Cd, Ni–MH, lead–acid batteries ...).

Moreover, several tests on Ni–Cd and Ni–MH electric vehicle modules and on one Li-ion MP cell, clearly demonstrate the interest of this technique for overcharge detection. In all cases, it has been possible to detect gas evolution, i.e., overcharge reactions. For electric vehicle battery modules, detection is either more efficient or comparable with other end-of-charge criteria such as temperature or voltage derivatives. For the Li-ion cell, results show that the noise power is proportional to a power of the gas evolution current fraction.

This study concerns whole battery voltage fluctuations without quantifying the contribution of each electrode. Another experimental set-up [15] has been defined for a better understanding of electrochemical noise sources in the batteries. This set-up allows the addition of two reference electrodes in a sealed Ni–MH battery. Thus, the electrochemical noise contribution of each battery component, positive electrode, negative electrode and battery separator, can be determined and explained [14].

References

[1] F. Job, PhD thesis, Institut National Polytechnique de Grenoble, Grenoble, 1979.
[2] C. Gabrielli, F. Huet, M. Keddam, J. Appl. Electrochem. 15 (1985) 503.
[3] C. Gabrielli, F. Huet, M. Keddam, A. Macias, A. Sahar, J. Appl. Electrochem. 19 (1989) 617.
[4] D.R. Hodgson, Electrochim. Acta 41 (1996) 605.
[5] P.C. Searson, J.L. Dawson, J. Electrochem. Soc. 135 (1988) 1908.
[6] C. Monticelli, G. Brunoro, A. Frignani, G. Trabanelli, J. Electrochem. Soc. 139 (1992) 706.
[7] F. Mansfeld, H. Xiao, J. Electrochem. Soc. 140 (1993) 2205.
[8] A. Legat, V. Dolecek, J. Electrochem. Soc. 142 (1995) 1851.
[9] U. Bertocci, C. Gabrielli, F. Huet, M. Keddam, J. Electrochem. Soc. 144 (1997) 31.
[10] U. Bertocci, C. Gabrielli, F. Huet, M. Keddam, P. Rousseau, J. Electrochem. Soc. 144 (1997) 37.
[11] F. Mansfeld, C.C. Lee, J. Electrochem. Soc. 144 (1997) 2068.
[12] C. Gabrielli, F. Huet, M. Keddam, Electrochim. Acta 31 (1986) 1025.
[13] P. Arora, R.E. White, M. Doyle, J. Electrochem. Soc. 145 (1998) 3647.
[14] S. Martinet, R. Durand, P. Ozil, P. Leblanc, P. Blanchard, to be submitted.
[15] S. Martinet, R. Durand, P. Ozil, P. Leblanc, P. Blanchard, 12th IBA Symposium, Grenoble-Annecy, 1998.